

Dynamic Response Characteristics of Layer Structure Slope Based On Transfer Function Analysis

Guo Li¹, Rui Fang¹, YaJun Li¹, Nengpan Ju²

¹*Broadvision Engineering consultants, National Engineering Laboratory for Surface Transportation Weather Impact Prevention, Kunming, Yunnan, China, 650041*

²*Key Laboratory of Geohazard Prevention and Geoenvironment Protection, Chengdu University of Technology, Chengdu, China, 610059*

Guo Li e-mail: ziltch2002@163.com

ABSTRACT

Through the shaking table test, this paper proposes a conclusion about the failure process of layer slopes under earthquake with different structures and lithology. Meanwhile, by using the transfer function of white noise signal input, the first modal damping of side slope model was deduced. The relationship between the damping ratio change and the model structure during the damage process of the model was analyzed. The test results indicate that the instability mechanism of four types of slope under earthquake can be concluded as: The hard rock bedding slope is caused by bedding slope drift - bottom collapse and bending instability. The hard rock anti-dipping slope is caused by trailing edge pull apart and middle-bottom part shear and slide type instability. The soft rock bedding slope results from bedding slope drift - bottom extrude - layer slip instability. The soft rock anti-dipping slope results from bending-located and shear type instability. Additionally, the dump change characteristic of the side slope model indicates that larger first modal damping changing happens in hard rock structure. As the earthquake becomes stronger, the damping of slope system will increase sharply in the development of failure surface. However, the damping ratio change characteristic of the soft rock slope is relatively gentle, which means the soft rock is less sensitive to the strength of the earthquake. The abrupt damping ratio change of the anti-dipping slope indicates the structural alternation of which is more obvious during an earthquake. Which gives a good explanation that why more earthquakes have occurred in hard rock slopes and why the earthquakes were stronger in anti-dipping slopes, as shown in 5.12 Wenchuan earthquake, 2008.

KEYWORDS: shaking table test, characteristic of dynamic response, instability mechanism, transfer function

INTRODUCTION

The dynamic response process of side slope can be regarded as the excitation and declination of new seismic wave during a shake spreading from the deep to the surface. So the material and the structure of the side slope are the main factors that influence the dynamic response characteristic. Because of the unpredictability of the earthquake wave, the vibration of authentic side slope is a random event, the factors such as waveform, frequency, amplitude, etc. cannot be acquired in advance. But the structural characteristic of the model itself is not. When the earthquake wave spreads through the slope, it will be affected by the inherent property slope such as the natural vibration frequency, damping, etc. and turn into a new one. In this process, how the earthquake wave change is only lies on the property of the side slope itself.

Table 1: Model Design Parameters

Lithology	Hard rock		Soft Rock	
	Prototype	Model	Prototype	Model
Density(kg/m ³)	26.5-27.5	27	26-27	26
E(MPa)	6000-9000	73.7	1000-3000	24.1
Poisson's ratio	0.25	0.25	0.28	0.28
Cohesion (MPa)	5-50	0.12	0.5-5	0.043
Friction angle (°)	38-45	43	30-38	35
Joint Cohesion (MPa)	0.5-1.0	0.006	0.05-0.5	0.001
Joint friction Angle(°)	35-40	37	25-30	25

Based on the similarity principle (Lai, 2005), models are built by barite powder, quartz sand, gypsum, glycerin, water, etc. The final material ratio is shown in Table 2.

Table 2: Model Material Ratio

Material(%)	Soft rock	Hard Rock
barite powder	51.3	43.2
quartz sand	32.1	30.9
gypsum	9	12.3
glycerin	6.4	8.6
water,	1.3	1.2
Engine oil	0	3.7

The experiment can get started when these four models built by the ratio above are on the shaking table (Fig. 2) and the pre-designed earthquake wave is loaded.

**Figure 2: Slope model placed on the shaking table**

EARTHQUAKE WAVE LOADING

Three types of earthquake waves will be loaded in this experiment, white noise, sine wave and the authentic earthquake wave respectively. In order to use the models effectively, authentic earthquake

wave loading will be increased step by step. After the working condition of each design being loaded, white noise signal with low amplitude is reloaded on the models.

Table 3: Working condition before white noise scanning

Condition	Amplitude(g)	earthquake wave	Sine wave
C01	0.05	/	/
C05	0.05		Z direction
C09	0.1		X direction
C16	0.1	0.1g	Z direction
C20	0.1		X direction
C24	0.1	0.2g	
C28	0.1	0.3g	
C32	0.1	0.4g	
C36	0.1	0.5	
C40	0.1	0.6	
C44	0.1	0.8	

Tips: Authentic earthquake wave should be loaded in the order of z/x/zx and the sine wave should be loaded in the order of 5/10/15HZ.

Macroscopical damage characteristic

Damage phenomenon of modelling experiment is the strongest evidence to proof instability mechanism and damage characteristic. After Wenchuan Earthquake, many scholars have done several shaking table tests. For instance, Xu, Q(2010) and Han-xiang, L's research(2011) of the slopes with hard upper and soft bottom structure and Dong Dong, J. Y's research(2011) of the bedding slopes whose slope angle is larger than their dip angle. These researchers have described the damage characteristic of side slopes systematically. In this test, if we regard the whole experiment as a complete earthquake process, the damage of the model can be regarded as a more and more stronger slope damage process under an earthquake wave.

In the experiment, when the earthquake wave was loaded under condition C46, the damage is obvious enough. Most of the sensors are damaged, and the model is completely damaged under condition C49. In order to guarantee the validity of the test data, the data which we have got after C46 was removed.

The experiment can be separated into 4 stages according to the strength of the earthquake wave.

Microearthquake stage: PGA value=0.1g.

Mid-amplitude earthquake stage: PGA value=0.2g to 0.3g.

Mid-Strong earthquake stage: PGA value=0.4g to 0.5g.

Strong earthquake stage: PGA value>0.5g.

Through recording and describing the damage of the four models under different conditions, we are able to know the macroscopical damage characteristics of the four models under seismic condition.

Hard Rock Bedding Slope

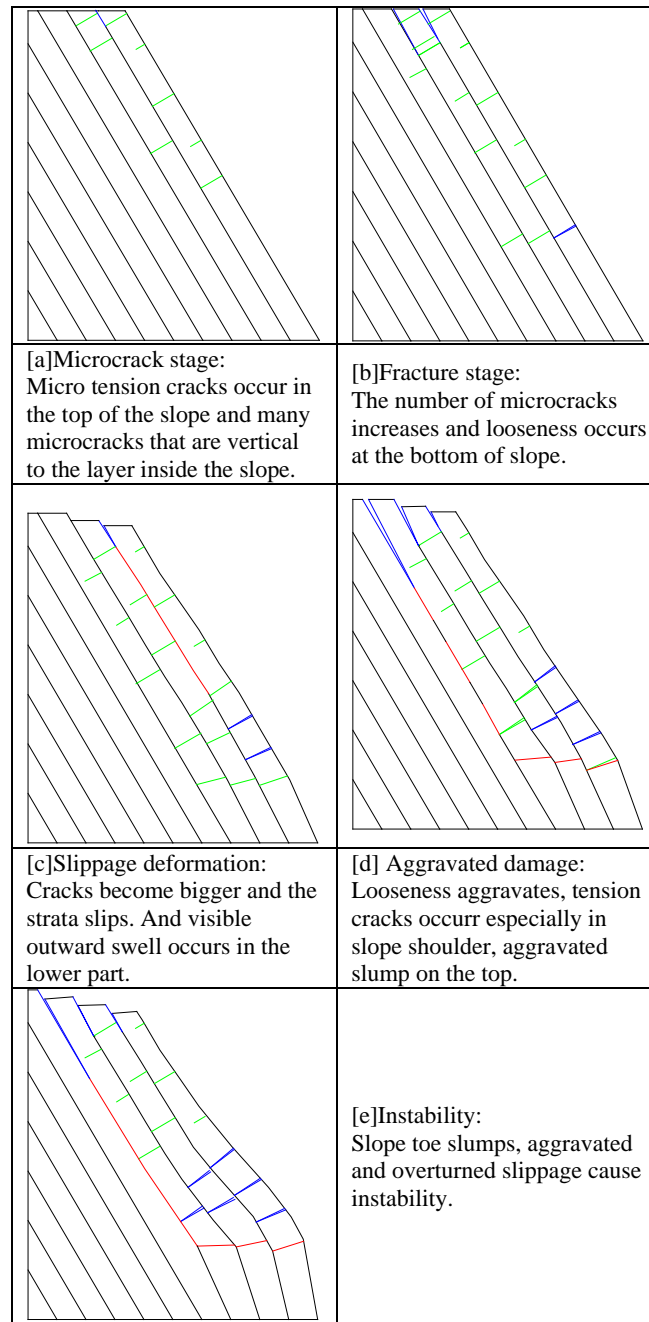


Figure 3: HD slope damage process

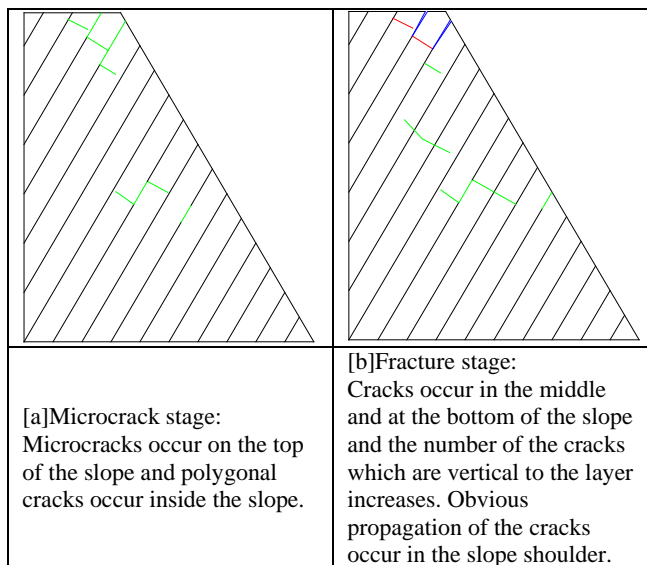
Instability mechanism of HD slope (Fig.3). Tension fracture, shear slippage and microcracks are shown as blue, red and green respectively, similarly hereinafter) can be described as: bedding foliation slippage - bottom collapse and bending instability. First of all, the earthquake makes the microcracks occur and the slope shoulder loosen. Secondly, with the increase of the earthquake strength, the cracks which are vertical to the layer surface develop. Finally, when the cracks spread

from the slope shoulder to the slope toe, uplift and collapse and bend (Fig.4) occur. Then the slope loses its stability.



Figure 4: Bend and collapse in slope toe

Hard Rock Anti-dipping Slope



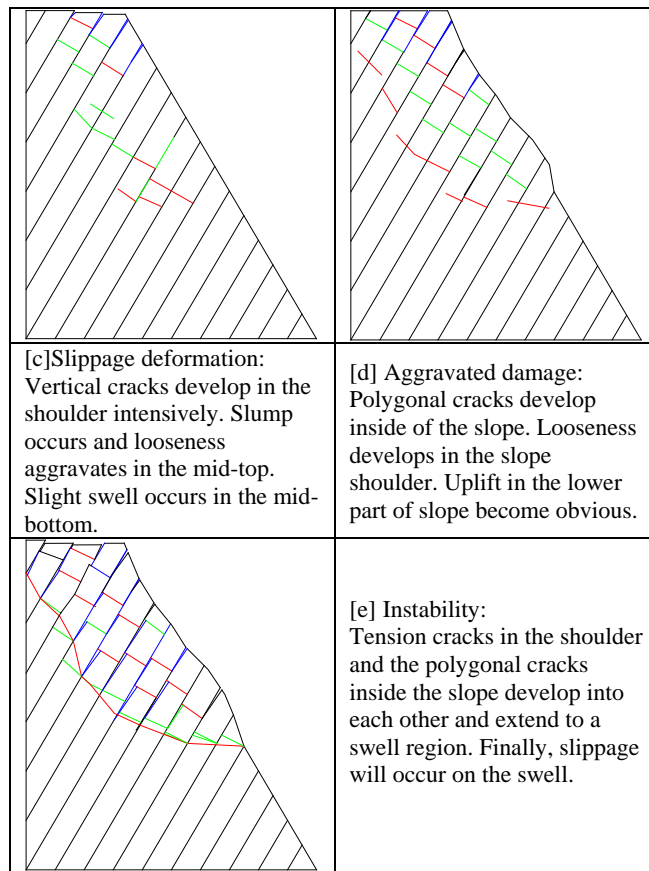


Figure 5: HAD slope damage process

The stability losing mechanism of HAD slope(Fig.5) is: trailing edge pull apart looseness—shear slipping stability losing. The damage starts by the development of tension crack on the slope surface. And then looseness and tension crack occurs. Then tension crack in the shoulder and the polygonal crack inside the slope develops into each other(Fig.6) and finally shear in the lower part of slope and then the slope loses stability.



Figure 6: polygonal crack inside the slope

Soft Rock Bedding Slope

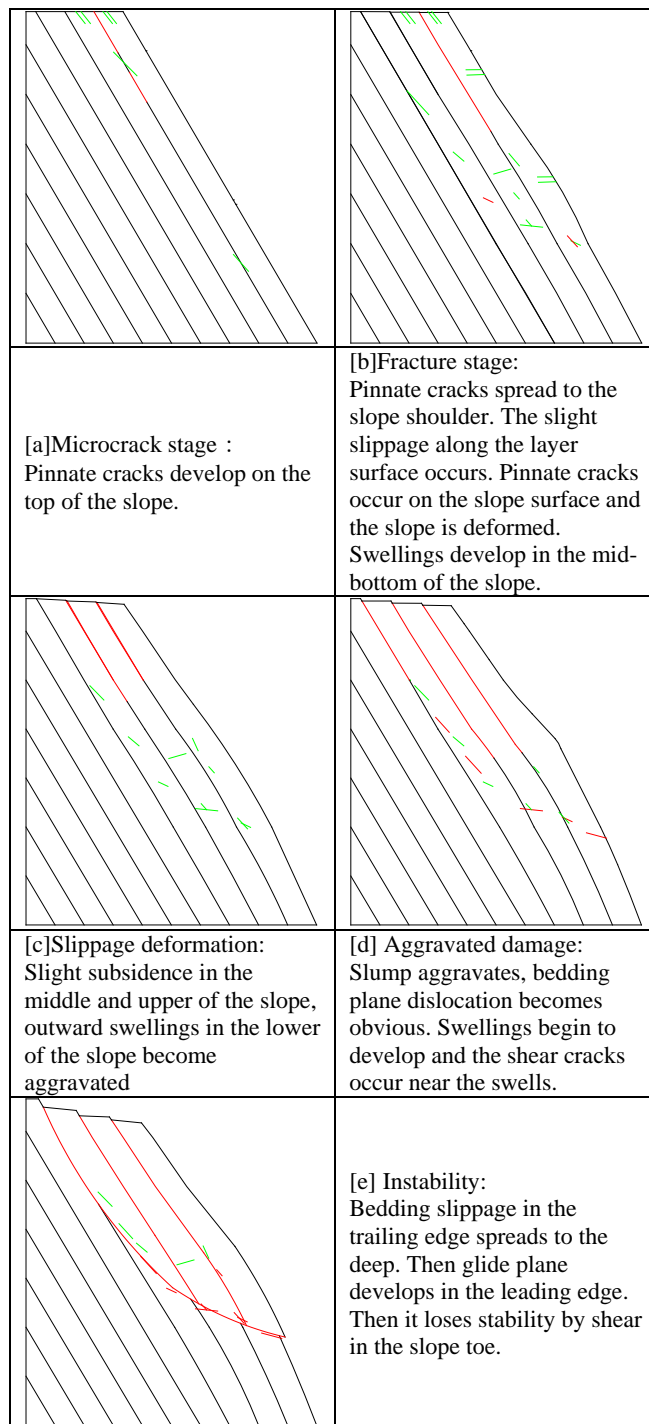


Figure 7: SD slope damage process

The instability mechanism of SD slope (Fig.7) is caused by bedding plane slippage - swells on the bottom - layered slippage damage. At first, rock and earth mass slips along the layer surface (Fig.8)

and deforms. Swells develop in the slope surface become obvious because of the deformation. The aggravated slippage of rock and earth mass in the mid-top and the aggravated swells finally make the layer surface shear. Then the whole slope lose stability corporately.

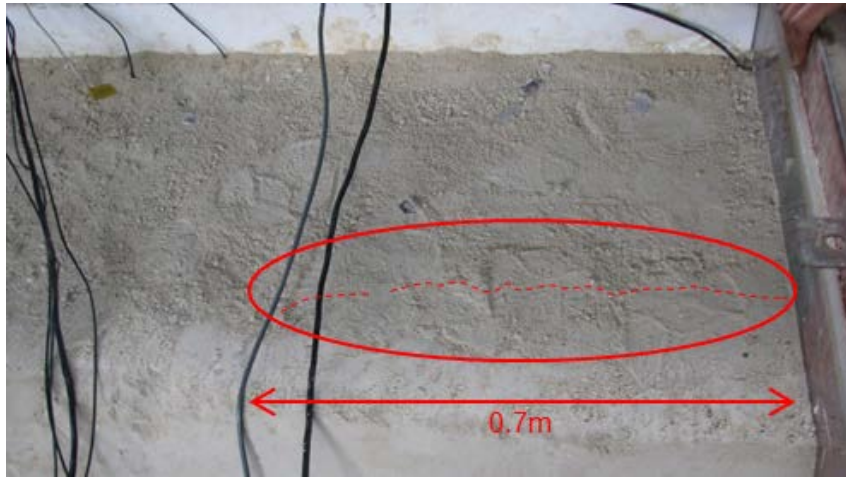
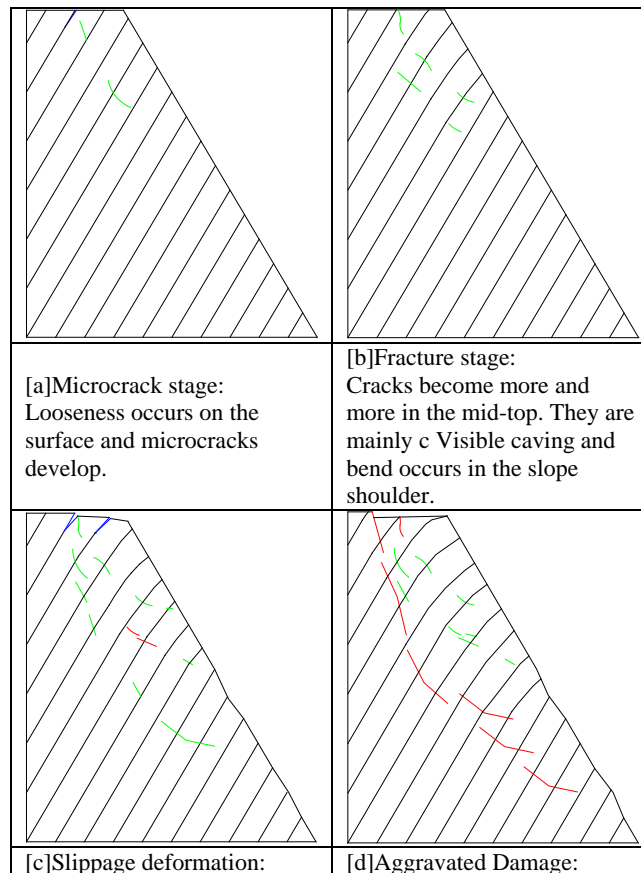


Figure 8: Slight slippage along the layer surface

Soft Rock Anti-dipping Slope



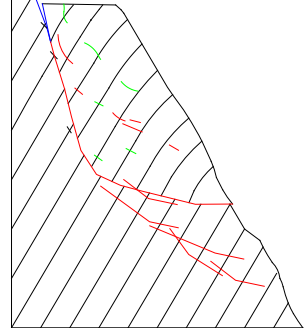
<p>Bend aggravates and the cracks vertical to the layer surface inside the slope become more and more. Obvious subsidence occurs in the slope shoulder. Swells develop in the middle and appear a potential sliding surface. Meanwhile, crack vertical to the layer surface occurs in the mid-bottom.</p>	<p>Bending and caving are aggravating. And cracks vertical to the layer surface become more and more. Then the cracks in the mid-bottom begin to hole. Swells in the slope toe is obvious.</p>
	<p>[e]Instability: Cracks in the trailing edge spread into the deep. The rock and earth mass on the top slumps. Instability occurs in mid-front.</p>

Figure 9: SAD slope damage process

The instability mechanism of SAD slope (Fig.9) is: Bending - shear instability. With the development of the cracks which are vertical to the layer surface by stratum bend, the bend on the top of the slope begin to hole gradually. Rock and earth mass in the leading edge is extruded. Finally, with the aggravation of bending and caving (Fig.10), the cracks in the trailing edge and the potential glide plane corporately cause instability by holing each other.



Figure 10: bending and caving in slope shoulder

Transfer function characteristics of model acceleration

Various earthquake waves are in the side slope modelling system. When the signals spread from the bottom to the top, the system would amplify the certain parts and other attenuate parts of the signal. So the signals will change when the wave is spreading through the system. And the change usually reflects the inner structure and dynamic characteristic of the side slope model. Thus, we can explain the inner rule during dynamic response of slope by studying the characteristics of the input and output signals.

Power spectral density and transfer function

The power spectral density (Buttkus, B, 2000) can analyze the signals submerged by noise in the region of frequency-domain. The method is appropriate to the model in this experiment when the white noise signal is loaded.

If the autocorrelation function of the random signal $x(t)$ is $R_x(\tau)$, then the Fourier transform of $R_x(\tau)$ is:

$$S_x(f) = \int_{-\infty}^{+\infty} R_x(\tau) e^{-j2\pi f\tau} d\tau \quad (1)$$

$S_x(f)$ is defined as the self-power spectral density or self-power spectrum of $x(t)$ because $S_x(f)$ can be explained as the distribution function of $x(t)$. The self-power spectrum $S_x(f)$ contains all the information of $R_x(\tau)$. If there is an component containing the certain frequency, it can be read from the self power spectrum.

If the self spectrum of the random signal is $S_x(f)$. Based on the Fourier inversion (Waser, J., & Schomaker, V., 1953), it can be obtained as:

$$R_x(\tau) = \int_{-\infty}^{\infty} S_x(f) e^{j2\pi f\tau} df \quad (2)$$

Similar to self power spectrum, the frequency characteristics of these two random signals $x(t)$ and $y(t)$ have cross-correlations. It can be described by cross-power spectrum density. Cross-power spectral density and the cross-correlation function are also Fourier transform spectrometer.

$$S_{xy}(f) = \int_{-\infty}^{\infty} R_{xy}(\tau) e^{-j2\pi f\tau} d\tau \quad (3)$$

$$R_{xy}(\tau) = \int_{-\infty}^{\infty} S_{xy}(f) e^{j2\pi f\tau} df \quad (4)$$

To discrete random sequence $x(n)$, the relationship between self-power spectral density $S_x(f)$ and autocorrelation function $R_x(m)$ is:

$$S_x(f) = \sum_{m=-\infty}^{\infty} R_x(m) e^{-j2\pi fmT_s} \quad (5)$$

where T_s is the data sample interval.

To discrete random sequences $x(n)$ and $y(n)$, the relationship between cross-power spectral density $S_{xy}(f)$ and cross-correlation function $R_{xy}(m)$ is:

$$S_{xy}(f) = \sum_{m=-\infty}^{\infty} R_{xy}(m) e^{-j2\pi f m T_s} \quad (6)$$

And

$$S_{xy}(-f) = S_{yx}(f), \quad S_x(f)S_y(f) \geq |S_{xy}(f)|^2 \quad (7)$$

The limitation of the signal length under the authentic conditions must be taken into consideration, so the self-power spectral density and the cross-power spectral density we use is an approximation of true value.

$$P_{xy}(\omega) = H(\omega)P_{xx}(\omega) \quad (8)$$

where P_{xx} is the self-power spectral density of $x(n)$. P_{xy} is the cross-power spectral density of $x(n)$ and $y(n)$. So the transfer function between the input $x(n)$ and output $y(n)$ can be approximated as:

$$\hat{H}(\omega) = \frac{\hat{P}_{xy}(\omega)}{\hat{P}_{xx}(\omega)} \quad (9)$$

Jiang, L.W. (2010) and Xu, G. (2008) have designed a group of experiments of soil mass models. They got a good achievement in the experiments by using the method of transfer function recognition. This paper will use the similar method to recognize and analyze the dynamic response characteristic of rock slopes in different structures.

Damping of side slope model and natural frequency characteristics of vibration

In every internal of earthquake wave loading, we input white noise signal with low amplitude, and deduce the transfer function between every acceleration recording point. The characteristic curves of typical acceleration transfer functions are shown as Figs. 11-14.

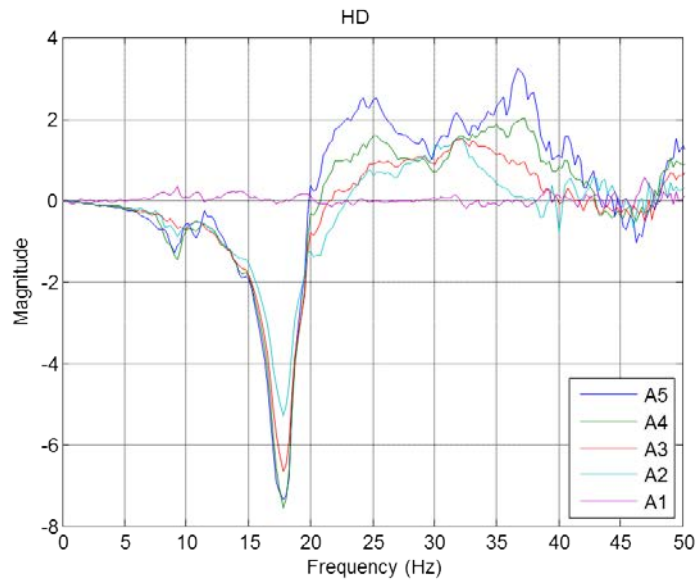


Figure 11: Transfer function of C01 HD slope test point under working condition

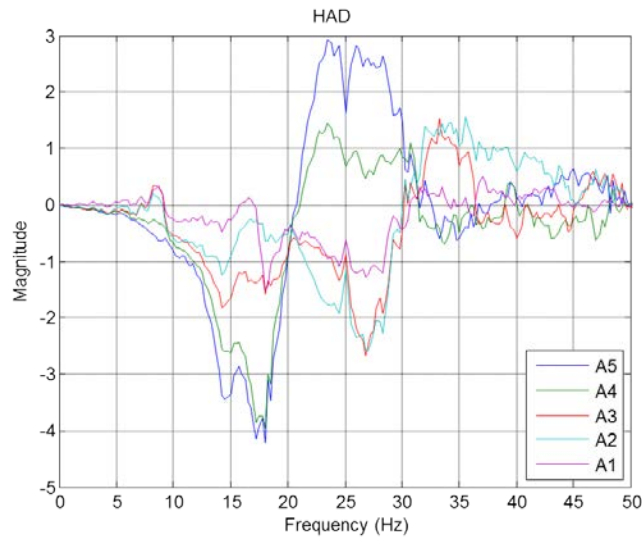


Figure 12: Transfer function of C01 HAD slope test point in working condition

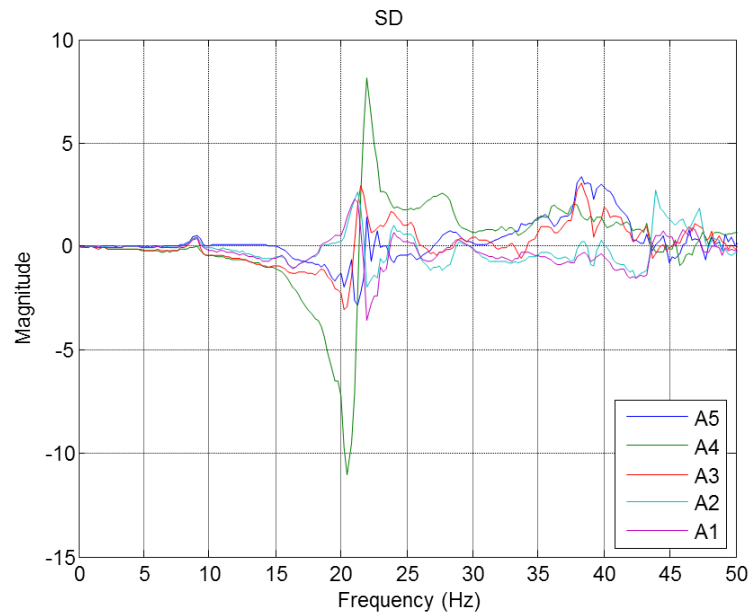


Figure 13: Transfer function of C01 SD slope test point under working condition

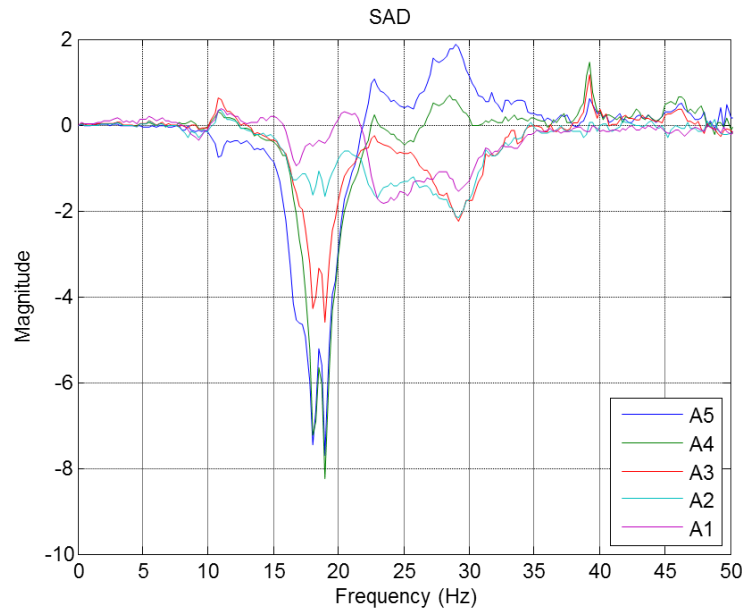


Figure 14: Transfer function of C01 SAD slope test point under working condition

By using the method in formula 9, all the transfer function characteristic curves under the white noise scanning working condition were recorded and the natural frequencies and corresponding modal damping were read. Then we can get the corresponding modal damping and natural frequency, as shown in Table 4.

Table 4: The conclusion of first order modal damping and natural frequency of vibration of the model system

Condition	HD		HAD		SD		SAD	
	Damping Ratio	Frequency (HZ)						
C01	0.076	17.74	0.149	17.97	0.031	21.23	0.074	18.99
C05	0.089	17.99	0.044	19.94	0.031	21.74	0.032	19.49
C09	0.088	17.68	0.166	17.99	0.043	21.99	0.085	18.23
C16	0.083	17.48	0.185	17.23	0.066	20.74	0.082	17.73
C20	0.104	16.73	0.208	14.49	0.064	17.28	0.055	17.23
C24	0.101	17.48	0.159	14.74	0.089	18.99	0.057	17.00
C28	0.108	17.23	0.208	14.50	0.085	17.98	0.061	16.73
C32	0.123	16.50	0.190	14.50	0.080	17.99	0.070	16.00
C36	0.151	16.48	0.146	14.58	0.057	19.24	0.073	15.00
C40	0.160	16.11	0.121	14.23	0.081	16.73	0.072	14.24
C44	0.172	15.49	0.123	13.99	0.078	16.50	0.119	12.50

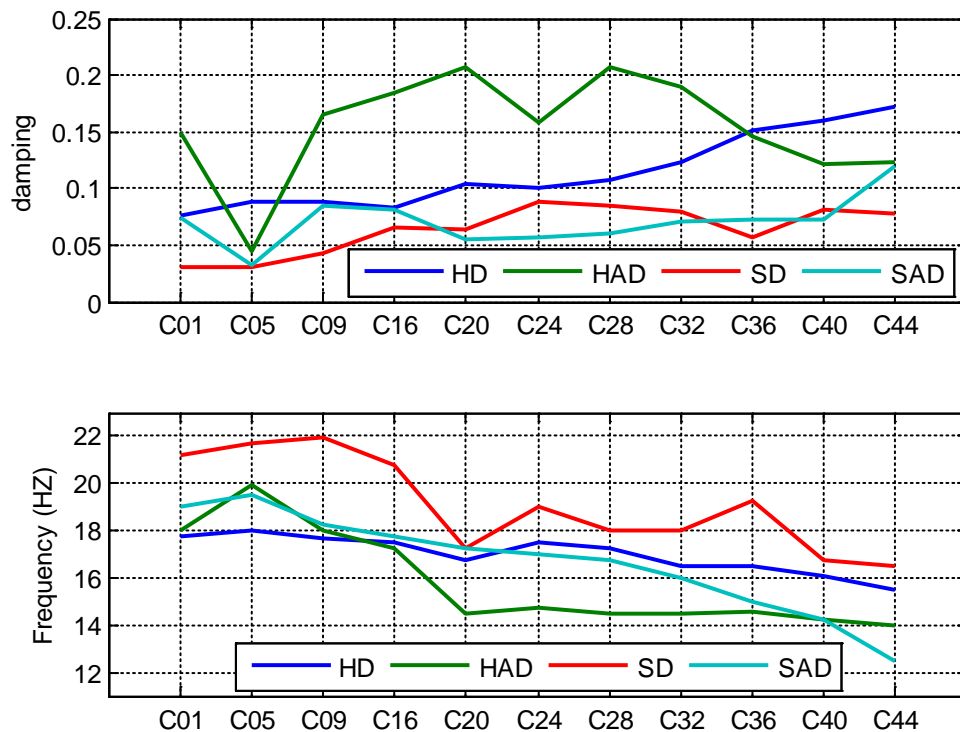


Figure 15: Tendency chart of characteristic frequency ratio and damping ratio of the side slope model

To draw a chart based on the data in Table 4, we can get the change curves of the frequency and damping ratio. As shown in Figure 15.

Obviously, the stronger the amplitude is, the larger the damping ratio of side slope system is and the lower the natural frequency of vibration is. This indicates that the stronger the earthquake is, the cracks inside the side slope are more aggravated. Therefore, the structure modal of the whole model is obviously deformed.

Additionally, the first order natural frequency of SD or SAD is higher than that of HD or HAD. To the slopes with the same lithology, the bedding slopes have a higher frequency than the anti-dipping slopes. In the vision of the damping change, the damping increase rate of SD is less obvious than that of HD. And the damping change curve of the anti-dipping slopes is getting stronger. However, that of the bedding slopes is gentle.

The rules above can explain the two characteristics of the disaster development in Wenchuan Earthquake(Huang R, 2013;Li G, 2011):

(1)More earthquakes occurred in HD slope.

When the earthquakes were getting stronger, the damage of HD structure was much worse than that of SD structure. The soft rock can do self-recovery and regenerate after being damage . But the hard rock cannot. The damage of hard rock usually was unrecoverable, and the damage would make a sudden increase to the damping of the structure, so that it would cause a worse damage.

(2)Anti-dipping slope often generated disaster of larger scale.

To bedding slope, the damage growth rate became faster with the strength of earthquake gradually. However, to the anti-dipping slope, the damage occurred suddenly. And the instability would make the intrinsic structure even worse. The damage was often in large scale and occurred suddenly.

CONCLUSION

The damping and natural frequency of vibration of the models in four types under different working conditions are calculated by using power spectral density and transfer function. The damage mechanism characteristics of the layer rock mass slope during the damage process of the side slope model are analyzed and discussed. The main conclusions are shown below.

(1) The damage characteristics and the difference of instability mechanism of four types of slope model (HD, HAD, SD, SAD) damage are closely related. The instability mechanism of hard rock bedding slope (HD) is due to the bedding slope drift - bottom collapse type curve instability, hard rock anti-dipping slope (HAD) is caused by the trailing edge pull apart and loose-middle and bottom shear and slide mode stability losing, soft rock bedding slope(SD) is caused by the bedding slope drift - bottom extrude - slip by layer, soft rock anti-dipping slope(SAD) is induced by the bending-located and shear mode instability.

(2) We use the transfer function to recognize the damping and frequency features of the slope. By these features, we can get the damping change characteristics during the earthquake. This method can be used to analyze the invisible model change during the process of the experiment.

(3) Various of damping characteristics are in the four types of models . Hard rock structure has a higher first order modal damping. And the damping will increase rapidly due to the strengthening of earthquake. Meanwhile, the damping of soft rock structure changes slowly. The damping anti-dipping

slope usually changes more suddenly than the bedding slope, so that the structure change is more obvious during the experiment process.

(4) By studying the damping change characteristics of the four types of slope models systemically, we can explain why the earthquake occurs more frequently in hard rock slope and why the earthquake in the anti-dipping slope is usually stronger.

ACKNOWLEDGMENT

The work in this paper was funded by National Natural Science Foundation of China, Yunnan United Fund: “Study on mechanical mechanism of landslide induced by environmental and engineering factors in Yunnan area”(No. U1402231).

REFERENCES

1. Agrahara Krishnamoorthy: “Factor of Safety of a Slope Subjected to Seismic Load” *Electronic Journal of Geotechnical Engineering*, 2007 (12.E). Available at ejge.com.
1. Buttkus, B. (2000). Spectral Analysis and Filter Theory in Applied Geophysics: With 23 Tables. Springer Science & Business Media.
2. El-Emam, M. M., & Bathurst, R. J. (2004). Experimental design, instrumentation and interpretation of reinforced soil wall response using a shaking table. *International Journal of Physical Modelling in Geotechnics*, 4(4), 13-32.
3. Dong, J. Y., Yang, G. X., Wu, F. Q., & Qi, S. W. (2011). The large-scale shaking table test study of dynamic response and failure mode of bedding rock slope under earthquake. *Rock and Soil Mechanics*, 32(10), 2977-2983.
4. Han-xiang, L. I. U., Qiang, X. U., & Hong-biao, X. U. (2011). Shaking table model test on slope dynamic deformation and failure. *Rock and Soil Mechanics*, 32(2), 334-339.
2. Hanumantha Rao Ch and G V Ramana (2015) “Site Specific Ground Response Analyses at Delhi, India” *Electronic Journal of Geotechnical Engineering*, 14(D):1-16.
3. Hassan Khosravi: “Parametric Analysis of Seismic Behavior of Two-Dimensional Triangular Shaped Hills in Time Domain” *Electronic Journal of Geotechnical Engineering*, 2015(20.4): 1243-1252. Available at ejge.com.
5. Huang, R., Li, G., Ju, N., & Zhao, J. (2013). Statistical Analysis of the Key Factors of Landslide Induced by Wenchuan Earthquake. In *Earthquake-Induced Landslides* (pp. 925-936). Springer Berlin Heidelberg.
6. Huang, R., Li, G., Ju, N., & Zhao, J. (2013). Statistical Analysis of the Key Factors of Landslide Induced by Wenchuan Earthquake. In *Earthquake-Induced Landslides* (pp. 925-936). Springer Berlin Heidelberg.
7. Iai S (1989) Similitude for shaking table tests on soil-structure fluid model in 1-g gravitational field. *Soils Found* 29(1):105–118
8. Iai, S., Tobita, T., & Nakahara, T. (2005). Generalised scaling relations for dynamic centrifuge tests. *Geotechnique*, 55(5), 355-362.

9. Liang-wei, J. I. A. N. G., Ling-kan, Y. A. O., & Wei, W. U. (2010). Transfer function analysis of earthquake simulation shaking table model test of side slopes. *Rock and Soil Mechanics*, 31(5), 1368-1374.
10. LI, G., HUANG, R., JU, N., & ZHAO, J. (2011). Study of distribution and development laws of secondary disaster in Longmenshan Area after earthquake. *Yangtze River*, 4, 009.
4. Lei Dongning, Wu Jianchao, Cai Yongjian, Li Heng, and Hu Qing: "Coseismic Coulomb Stress Change of Japan Mw9.0 Earthquake and Triggering of Aftershocks" *Electronic Journal of Geotechnical Engineering*, 2015(20.4): 1243-1252. Available at ejge.com.
5. Waseim Ragab Azzam: "Seismic Response of Bucket Foundation and Structure Under Earthquake Loading" *Electronic Journal of Geotechnical Engineering*, 2014 (19.F) pp 1477-1489. Available at ejge.com.
11. Waser, J., & Schomaker, V. (1953). The Fourier inversion of diffraction data. *Reviews of Modern Physics*, 25(3), 671.
12. Xu C, Shyu JBH, Xu XW (2014a) Landslides triggered by the 12 January 2010 Port-au-Prince, Haiti, Mw = 7.0 earthquake: visual interpretation, inventory compiling, and spatial distribution statistical analysis. *Nat Hazards Earth Sys* 14(7):1789–1818
13. Xu, Q., Liu, H., Zou, W., Fan, X., & Chen, J. (2010). Large-scale shaking table test study of acceleration dynamic responses characteristics of slopes [J]. *Chinese Journal of Rock Mechanics and Engineering*, 12, 009.
14. Xu, G. X., Yao, L. K., Gao, Z. N., & Li, Z. H. (2008). Large-scale shaking table model test study on dynamic characteristics and dynamic responses of slope. *Chinese Journal of Rock Mechanics and Engineering*, 27(3), 624-632.
6. Zheng Qingtao, Zhao Yamin, and Wang Wei: "Statistical Characteristics of 1966-2015 Shallow Earthquake Sequences with $M \geq 6.0$ in Mainland China" *Electronic Journal of Geotechnical Engineering*, 2016 (21.09) pp 3137-3151. Available at ejge.com.



© 2016 ejge

Editor's note.

This paper may be referred to, in other articles, as:

Guo Li, Rui Fang, YaJun Li, Nengpan Ju: " Dynamic Response Characteristics of Layer Structure Slope Based On Transfer Function Analysis" *Electronic Journal of Geotechnical Engineering*, 2016 (21.12), pp 4135-4452. Available at ejge.com.